Astron. Astrophys. 333, 31–37 (1998)

ASTRONOMY AND ASTROPHYSICS

BeppoSAX observations of narrow-line Seyfert 1 galaxies

I. Ton S 180

A. Comastri[1], **F. Fiore**[2,3], **M. Guainazzi**[3], **G. Matt**[4], **G.M. Stirpe**[1], **G. Zamorani**[1], **W.N. Brandt**[5], **K.M. Leighly**[6], **L. Piro**[7], **S. Molendi**[8], **A.N. Parmar**[9], **A. Siemiginowska**[10], **and E.M. Puchnarewicz**[11]

[1] Osservatorio Astronomico di Bologna, Via Zamboni 33, I-40126 Bologna, Italy
[2] Osservatorio Astronomico di Roma, Via dell'Osservatorio, I-00040 Monteporzio-Catone, Italy
[3] SAX-Science Data Center, Nuova Telespazio, Via Corcolle 19, I-00131 Roma, Italy
[4] Dipartimento di Fisica "E. Amaldi", Università degli Studi "Roma Tre", Via della Vasca Navale 84, I-00146 Roma, Italy
[5] Department of Astronomy and Astrophysics, The Pennsylvania State University, 525 Davey Lab, University Park, PA 16802, USA
[6] Department of Astronomy, Columbia University, 538 West 120th Street, New York, NY 10027, USA
[7] Istituto di Astrofisica Spaziale – C.N.R., via E. Fermi 21, I-00044 Frascati, Italy
[8] Istituto di Fisica Cosmica e Tecnologie Relative – C.N.R., via Bassini 15, I-20133 Milano, Italy
[9] Astrophysics Division, Space Science Department of ESA ESTEC/SA, 2200 AG Noordwijk, The Netherlands
[10] Harvard-Smithsonian Center for Astrophysics, 60 Garden St., Cambridge, MA 02138, USA
[11] Mullard Space Science Laboratory, University College London, Holmbury St. Mary, Dorking, Surrey RH5 6NT, UK

Received 9 September 1997 / Accepted 9 December 1997

Abstract. We report on the first spectrum up to 10 keV of the bright narrow-line Seyfert 1 galaxy Ton S 180, obtained with the imaging instruments onboard BeppoSAX. This is the first observed source in a sample of a dozen narrow-line Seyfert 1 galaxies in the BeppoSAX Core Program. We also present and discuss a high quality optical spectrum taken at the 1.5 m telescope at La Silla two months before the BeppoSAX observation.

The X-ray spectrum shows a clear hardening above about 2 keV, where a power law with $\Gamma \simeq 2.3$ plus an iron line provide a good description of the data. This slope is significantly steeper than the typical one for classical Seyfert 1's and quasars. The best fit line energy is suggestive of highly ionized iron, which would support the idea that the high accretion rate is (one of) the fundamental parameter(s) characterizing the Narrow Line Seyfert 1 phenomenon.

Key words: X-rays: galaxies – galaxies: Seyfert – galaxies: individual: Ton S 180

1. Introduction

Narrow-line Seyfert 1 galaxies (hereafter NLS1; see Osterbrock & Pogge 1985) are defined by their optical emission line properties. They lie at the lower end of the broad line width distribution for the Seyfert 1 class with typical values of the Hβ FWHM in the range 500–2000 km s^{-1}. The [O III]/Hβ ratio is < 3, and strong Fe II, Ca II triplet $\lambda 8498$, $\lambda 8542$, $\lambda 8662$ and O I $\lambda 8446$ emission lines as well as high ionization lines typical of Seyfert 1 galaxies are common among these objects. A remarkable and extremely strong anti–correlation was found between ROSAT PSPC X-ray spectral slope (0.1–2.0 keV) and the Hβ FWHM (Boller et al. 1996, hereafter BBF96; Forster & Halpern 1996; Grupe 1996; Laor et al. 1997). Steep soft X-ray spectral slopes with typical photon indices (derived from single power-law fits) in the range $\Gamma \simeq 3$–5 are only found among objects with narrow optical permitted lines.

Large-amplitude and rapid X-ray variability is common among NLS1. Moreover, there is evidence for giant-amplitude X-ray variability (up to about two orders of magnitude) in IRAS 13224–3809 (Boller et al. 1993, 1997; Otani et al. 1996), PHL 1092 (Forster & Halpern 1996), RE J 1237+264 (Brandt et al. 1995; Grupe et al. 1995a) and WPVS007 (Grupe et al. 1995b). It is notable that such extreme variability properties have been discovered, so far, only in NLS1.

In the harder $\approx$ 2–10 keV energy band, recent ASCA observations have shown that NLS1 can have very different behaviour from classical broad-lined Seyfert 1s and quasars. A comparative ASCA study of a large sample of NLS1 and broad-line Seyfert 1s revealed that the $\approx$ 2–10 keV ASCA spectral slopes of NLS1 are generally steeper than those of broad line objects at a high statistical confidence level (Brandt et al. 1997).

In order to increase the statistics of hard X-ray data for NLS1 galaxies we have undertaken a program of BeppoSAX observations of a sizeable sample of NLS1 (about 12 over 3 years). We have selected, for the first year of observations, among the brightest and most variable NLS1 previously observed by ROSAT and/or ASCA. The spectral capabilities of the detectors onboard BeppoSAX and especially the relatively large effective area at high energy (> 2 keV) will allow a better study of the high energy properties of NLS1.

Send offprint requests to: A. Comastri
(e-mail: comastri@astbo3.bo.astro.it)

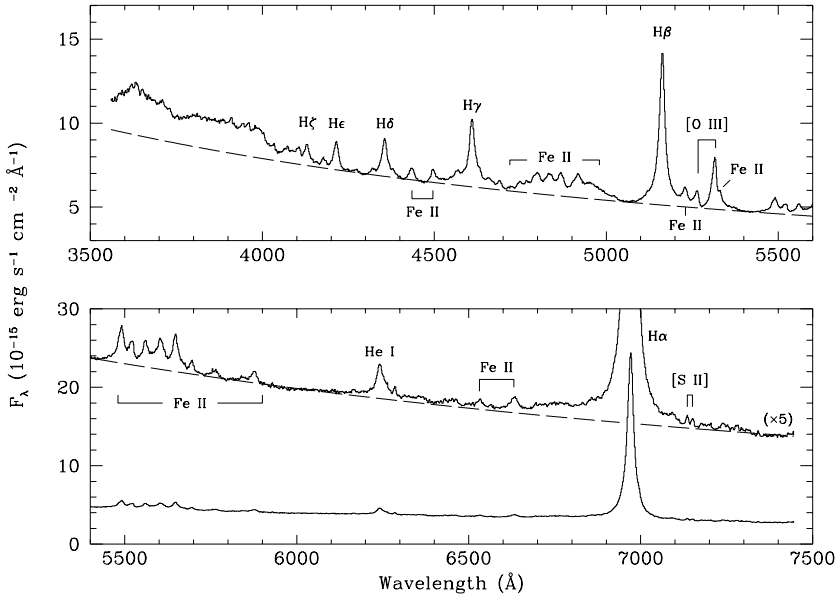

Fig. 1. The optical spectrum of Ton S 180 obtained at ESO in 1996 October. The spectrum has been split in two segments for viewing purposes. The bottom panel also shows the red segment scaled up by a factor 5, in order to show the weaker lines. The main emission lines are indicated on the figure. The dashed line is the fitted power-law continuum (see text). The wavelength scale is in the rest system of the observer (z=0.062)

In this paper we present the first simultaneous 0.1–10 keV spectrum of the narrow-line quasar Tonantzintla S 180 (hereafter Ton S 180) obtained with the BeppoSAX satellite, together with a high-quality optical spectrum obtained at La Silla two months before the X-ray observation.

Ton S 180 is an optically bright (V = 14.4) galaxy with an optical spectrum typical of NLS1 at z = 0.062. Multicolor UBVRI photometry revealed small amplitude variations on the order of 0.1 mag over a timescale of a few months (Winkler et al. 1992). It is also a relatively bright extreme ultraviolet (EUV) source detected by the EUVE satellite with a flux density $\nu F_\nu \sim 3.9 \cdot 10^{-11}$ erg cm^{-2} s^{-1} at 0.14 keV assuming a power law spectrum of photon index Γ = 2.4 and Galactic absorption (Vennes et al. 1995). Large amplitude EUV variability has been also detected with a doubling time of about 12 hours (Hwang & Bowyer 1997).

Several PSPC observations, both from the ROSAT All-Sky Survey and the ROSAT pointed program, have been discussed by Fink et al. (1996). The soft X-ray flux shows variability with an amplitude up to a factor of ≈ 2 on time scales ranging from hours to days and years. The intensity variations are not clearly associated with significant spectral variations. The $\sim$ 0.1–2.4 keV spectrum is steep, with photon index values ranging between $\sim$ 2.7 and 3.2. When averaged over all the observations the mean PSPC spectrum is well represented by a two component model consisting of a power law with $\Gamma = 3.10 \pm 0.05$ and a very steep low energy component, dominant below 0.3 keV, which can be represented either as a steeper power law or as blackbody emission at low temperature ($\sim 16 \pm 3$ eV).

2. The optical spectrum

2.1. Observations and reduction

Optical spectra of Ton S 180 were obtained at the ESO 1.52m telescope on 1996 October 1 and 2, using the Boller & Chivens spectrograph with a 127mm camera and a Loral/Lesser thinned CCD with 2048×2048 pixels. The pixel size is 15μm, and the projected scale on the detector is 0.82 $''$ pixel^{-1}. The grating used had 600 grooves mm^{-1}. The spectra were obtained through a 2 $''$ wide slit at a resolution of 4.6 Å. Both nights were photometric. Four integrations of 1800 seconds each were obtained.

Standard techniques were used to reduce the spectra, using the NOAO IRAF package. In particular, the spectrophotometric calibration of the spectra was perfected by comparison with short exposures of Ton S 180 obtained during the same nights through an 8 arcsec slit. This allowed us to correct the narrow-slit spectra for light losses and differential refraction. The four individual spectra were finally averaged and yielded the final spectrum shown in Fig. 1. Because the calibration curves of the two nights and the individual spectra coincide within $<$5%, we consider the spectrophotometric quality of the final spectrum to be of this order.

2.2. Properties of the optical spectrum

The spectrum of Ton S 180 presents characteristics normally associated with NLS1, such as strong Fe II multiplets and a weak narrow-line spectrum. The only clearly visible forbidden lines are [O III]λ5007 and λ4959, while [S II]λ6717 and λ6731 are barely detected (Fig. 1). There is no detection of other forbidden lines, such as those of [N II], [O I], and [Fe VII], which are usually clearly visible in Seyfert spectra. The broad line spectrum of Fe II, on the other hand, with the individual lines of multiplets 27, 28, 37, 38, 42, 43, 46, 48, 49, 55, and 74 is clearly visible (compare with Phillips 1976).

The continuum redwards of ~ 4300 Å is well represented by a power-law function with slope $\alpha = -1.7$, where $F_\lambda \propto \lambda^\alpha$, corresponding to $F_\nu \propto \nu^{-0.3}$. The estimate of α was obtained by fitting a power-law to several dips in between the emission lines. Fig. 1 includes the fitted continuum. The strong excess emission at short wavelengths is part of the well-known small

Table 1. Fluxes and widths of the main optical emission features

Feature[a]	Flux[b]	FWHM[c]
Fe II λ4570 blend	2.2	...
Hβ	2.6	1120
$[OIII]\lambda5007$	0.6	860
Fe II λ5250 blend	1.1	...
He I λ 5876	0.2	1100
Hα	7.1	950

[a] All wavelengths are in rest frame
[b] Units of 10^{-13} erg cm^{-2} s^{-1}
[c] km s^{-1}

blue bump, which is centred at a rest wavelength of $\sim$ 3300 Å and is most likely the result of a blend between the Balmer continuum and several Fe II multiplets.

The high signal-to-noise ratio of the spectrum allows to detect very broad, low-intensity wings under Hα, covering the $\sim$ 6600–7150 Å range. Rodríguez-Pascual et al. (1997) have recently presented evidence for the presence of broad wings in the UV lines of a sample of NLS1 (which however did not include Ton S 180): there is therefore a possibility that similar components are present in the optical permitted lines (note however that Rodríguez-Pascual et al. searched for broad wings under Hα in two objects of their sample without detecting them). While we do not exclude this possibility, we are also concerned that the feature, which is very blue-asymmetric, may be caused by the presence of Fe II multiplets bluewards of Hα. Some lines of multiplet 74, in particular, are clearly visible. In addition a local deviation of the continuum from the chosen power-law may contribute to creating a spurious wing. More detailed discussion and analysis of this feature are deferred to a future paper.

Table 1 lists the integrated fluxes of the main lines, derived by integrating the flux above a continuum fitted to the local minima close to the measured emission features. The strength of the Fe II blends relative to Hβ, while not as high as that of I Zw 1, the prototypical NLS1, is nevertheless much higher than that typical for normal Seyfert 1 nuclei (Joly 1988).

The fluxes of Hβ and [O III]λ5007 were measured after subtraction of the strongest blending lines with suitable templates. Fe II λ4924 and Fe II λ5018 were subtracted by using the profile of Hα scaled by a factor 0.04, under the reasonable assumption that the lines in multiplet 42 are of equal intensity. The scaling factor was chosen visually by trial and error, on the basis of the smoothest residual spectrum. To subtract [O III]λ4959 we used the deblended profile of [O III]λ5007 scaled by one third. The ratio of Hα and Hβ (2.7) is one of the lowest observed in a type 1 AGN. According to photoionization models based on typical properties inferred for the broad-line region (BLR), and as low densities are excluded because of the relative narrowness of the [O III] lines, this may imply that densities in the BLR of Ton S 180 are higher than $\sim 10^{11}$ cm^{-3} (e.g. Rees et al. 1989, Zheng & Puetter 1990).

3. BeppoSAX data reduction

The X-ray satellite BeppoSAX (Boella et al. 1997a), a program of the Italian Space Agency (ASI) with participation of the Netherlands Agency for Aereospace Programs (NIVR), includes four co–aligned Narrow Field Instruments (NFI): a Low Energy Concentrator Spectrometer (LECS; Parmar et al. 1997), three Medium Energy Concentrator Spectrometers (MECS; Boella et al. 1997b), a High Pressure Gas Scintillation Proportional Counter (HPGSPC), and a Phoswich Detector System (PDS). The LECS and MECS have imaging capability and cover the 0.1–10 keV and 1.3–10 keV energy ranges respectively; in the overlapping band the total effective area of the MECS (which is $\sim$150 cm^2 at 6 keV) is about three times that of the LECS. The energy resolution is $\sim$8%, and the angular resolution is $\sim$1.2′ (Half Power radius) at 6 keV for both instruments.

BeppoSAX observed the source with the NFI on 1996 December 3 for about 25 ks effective time with MECS and 12 ks with LECS. The shorter LECS exposure is due to the switching off of the instrument over the illuminated Earth. The HPGSPC and the PDS were not sensitive for this rather faint source, and thus data are presented only for LECS and MECS.

LECS spectra have been extracted from a 9′ radius region around the centroid of the source image, which allows the collection of about $\sim$ 95% of the photons in the carbon band (E $<$ 0.3 keV). For the MECS the adopted extraction radius was 4′. The source radial profiles in both the LECS and MECS are consistent with those expected from the PSF without any evidence of extended X-ray emission. The spectra from the three units have been equalized to the MECS1 energy–PI relationship and added together. Since the MECS background is very low and stable[1], we used all data acquired with an angle, with respect to the Earth's limb, higher than 5°.

We are interested in the high energy spectrum of this source and since it is rather faint, and possibly very steep, background subtraction plays a crucial role. Background counts were accumulated from regions surrounding the sources and compared with counts accumulated from the same regions from blanksky observations. The 'local' and 'blank sky' background counts were always within 10% of each other for the three MECS detectors and for the LECS. We used in our spectral analysis the 'blank sky' background extracted from the 'blank sky' event files in the same regions as the source.

The background subtracted count rates are 0.127 $\pm$ 0.004 cts s^{-1} for LECS in the 0.1–6 keV band and 0.096 $\pm$ 0.002 cts s^{-1} for the 3 MECS in the 1.5–10 keV energy range.

4. Timing analysis

Fig. 2 shows the background subtracted light curves over the 0.1–3 keV (LECS) and 3–10.5 keV (MECS) energy ranges. The time shown in the X axis is computed from the beginning of the observation. The source data have been extracted from a circular region with a 4 arcmin radius for both instruments. The

[1] For information on the background and on data analysis in general see *http://www.sdc.asi.it/software/cookbook*

background, derived from an outer region at about 10 arcmin from the center in the same observation, has been corrected for an average vignetting correction estimated from the analysis of a deep observation of a blank sky area. The background contribution to the total counts in the 4 arcmin region is $\sim 5\%$ in the LECS and $\sim 13\%$ in the MECS data.

The data points shown in Fig. 2 correspond to periods of continuous observation. The length of the observation in each orbit is indicated by the horizontal lines, while the vertical lines show the 1σ statistical uncertainty. Both light curves show significant variability, of the order of a factor of two, during the length of the entire observation. The hypothesis of a constant count rate can be rejected with a high level of confidence in both the 0.1–3.0 keV ($p < 1 \cdot 10^{-5}$) and 3.0-10.5 keV ($p \sim 8 \cdot 10^{-4}$) energy ranges. No significant variability is instead detected within the data from single orbits (i.e. on timescales of the order of 1,000 – 3,000 s).

Visual inspection of the two light curves suggests the possibility that, during the increase of the source flux (at t $\sim$ 10,000 s), the hard curve lags the soft one. In fact, the peak in the MECS data is seen at t $\sim$ 17,000 s, while the correponding peak in the LECS data is seen at t $\sim$ 12,000 s. However, the significance of this effect is only marginal and data with better statistics and/or with a more continuous time coverage would be needed to reliably conclude that this time lag is real. For example, the two solid lines in Fig. 2 show two light curves which, having been obtained by keeping fixed the ratio between LECS and MECS counts (i.e. with no spectral variation), are however consistent at better than 2σ with both the LECS and MECS data. The same conclusion is reached by analyzing the hardness ratio, defined as the ratio between the MECS and LECS counts, as a function of time. Therefore, since the data are consistent with a spectrum which changes only in normalization, in the next section we will derive the shape parameters for the spectrum using the data averaged over the entire observation.

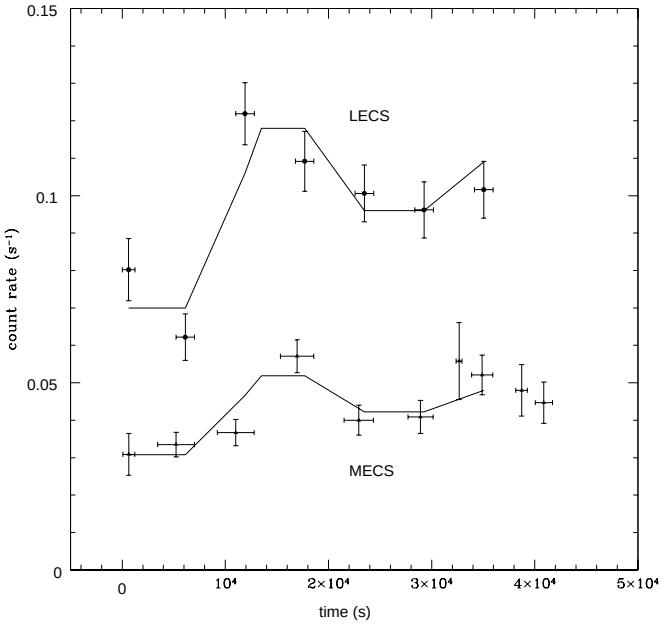

Fig. 2. Background subtracted LECS (0.1–3 keV) and MECS (3–10.5 keV) light curves, obtained from a circular region with a 4 arcmin radius for both instruments. The meaning of the two solid lines is described in the text

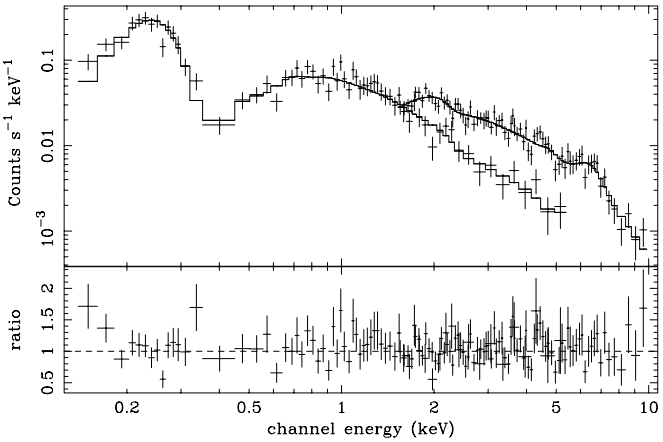

Fig. 3. The LECS + MECS spectrum of Ton S 180. The energy scale is in the rest system of the observer. See the text for the spectral model that has been fitted to the data

5. Spectral analysis

5.1. The 0.1–10 keV spectrum

For the spectral analysis the source counts have been grouped with a minimum of 20 counts per energy bin in the $\sim$ 0.1–6 keV (LECS) and $\sim$ 1.5–10 keV (MECS) energy ranges. The LECS and MECS datasets have been fitted simultaneously with the relative normalizations free to vary, in order to take into account the different exposure times and the relative calibration of the two instruments (Cusumano et al. in preparation) The spectral fits have been performed with the XSPEC 9.0 fitting package, using the response matrices released on Jan 1997. In the following, all quoted errors correspond to the 90% confidence level. A summary of the results is reported in Table 2.

The first line of Table 2 shows the parameters obtained for the best fit model. This model, computed by keeping the N_H value fixed at the Galactic value measured in the direction of Ton S 180 ($(1.5 \pm 0.5) \times 10^{20}$ cm^{-2}; Dickey & Lockman 1990), is characterized by two power laws, with best fit slopes Γ_s = 2.68 and Γ_h = 2.29, plus a narrow ($\sigma \equiv 0.01$ keV) gaussian line centered at 7.11 ± 0.16 keV with an equivalent width of 507 ± 247 eV. The resulting fit (χ^2 = 135 with 135 degrees of freedom) is shown, superimposed on the data, in the upper panel of Fig. 3. The lower panel, showing the ratio between data and model, clearly indicates that this model is a good representation of the data over the entire energy range. Similar results are obtained by leaving the N_H value free to vary, with a best fit value of $N_H = (1.15 \pm 0.45) \times 10^{20}$ cm^{-2}, consistent with the galactic value. Substituting the power law at low energy with a blackbody emission produces a significantly worse fit quality ($\Delta\chi^2$=8.1 with the same number of degrees of freedom; see second line in Table 2).

The line energy is consistent at the 90% level with a hydrogen–like iron line at 6.97 keV. Leaving the width σ of

the line free to vary the improvement in the fit quality is only marginal ($\Delta\chi^2 \simeq 2.5$). The formal width is ~ 0.5 keV and the gaussian centroid is ~ 6.9 keV. The best fit line energy is therefore suggestive of a highly ionized accretion disk. A characteristic strong feature from such a disk is expected to be a smeared iron absorption edge (e.g. Ross et al. 1996), but this feature is not seen in the present data. Alternatively, the ~ 7.1 keV line could be the blue horn of a relativistic disk line from an edge–on disk, rather than a ionized one. To test this possibility we have fitted the diskline model in XSPEC to the observed spectrum. Unfortunately, even though an acceptable description of the data can be obtained with a disk line, the quality of the present data does not allow us to put strong constraints on the inclination angle.

We have also tried to model the soft X-ray spectrum below ~ 2 keV with more complex models fixing the absorption at the Galactic value. Both an ultrasoft blackbody plus a power law and a double blackbody (which would be a first–order approximation of the accretion disk emission) provide acceptable descriptions of the soft X-ray spectrum. However, they are not statistically required by the present data.

On the basis of the best fit model, the unabsorbed 0.1–2.0 keV flux is $\sim 3 \cdot 10^{-11}$ erg cm^{-2} s^{-1}, corresponding to a soft X-ray luminosity of $\sim 5.3 \cdot 10^{44}$ erg s^{-1} (H_0 = 50 km s^{-1} Mpc^{-1}; q_0 = 0). This places Ton S 180 among the X-ray luminous quasars. The soft X-ray flux is almost an order of magnitude greater than the observed 2–10 keV flux of $\sim 4.2 \times 10^{-12}$ erg cm^{-2} s^{-1}, which corresponds to a 2–10 keV luminosity of $\sim 7.4 \cdot 10^{43}$ erg s^{-1}.

Simpler models (i.e. with a smaller number of free parameters) do not adequately fit the data over the entire range of energy. This is shown in the next two lines of Table 2, which give the best fit parameters and the χ^2 values of the fits for a model with two power laws and no emission line (third line in Table 2) and a single power law with emission line (fourth line in Table 2). In both cases, the quality of the fit, as judged by the increase in the χ^2 value, is significantly worse than that obtained for our best fit model. In the first case a clear excess in the residual is present around 6–7 keV (Fig. 4); in the second case systematic residuals both at low and high energies are left, moreover the extremely high value found for the iron line equivalent width also suggest a rather poor approximation of the continuum at energies $>$ 5–6 keV.

5.2. Comparison with ROSAT results

The direct comparison of the spectral analysis results with those obtained by Fink et al. (1996) is not straightforward given the source variability and the different assumptions about the continuum model between ROSAT and BeppoSAX. The range of PSPC spectral slopes is in good agreement with the power-law fits of the soft component reported here (Table 2). This suggests that the slope of the soft X-ray spectrum remains steep on timescales of several years, while the soft flux undergoes significant and rapid variations. The unabsorbed 0.1–2.4 keV flux of 2.6 $\cdot 10^{-10}$ erg cm^{-2} s^{-1}, derived by Fink et al. (1996) on the basis of a two component model consisting of an ultra–soft blackbody plus a steep power law, is almost an order of magnitude greater than the present measurement. While this could be due, at least in part, to the different adopted spectral parameters and in particular to the larger value of the column density derived by Fink et al. (1996), it is likely that Ton S 180 was, on average, brighter during the ROSAT observation. The derived flux density at 0.14 keV of 1.5–1.8 $\cdot 10^{-11}$ erg cm^{-2} s^{-1}, depending on the assumed spectral model, is more than a factor 2 lower than that obtained by EUVE (Vennes et al. 1995), for a similar assumption on the spectral parameters, confirming large amplitude flux variability.

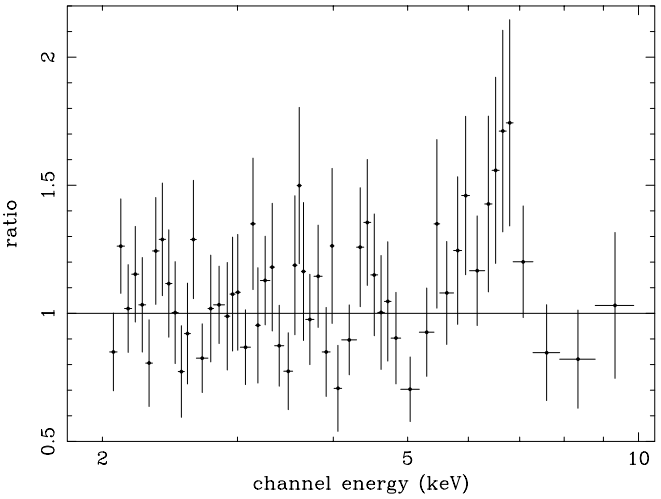

Fig. 4. Residuals from a single power law fit ($\Gamma = 2.21 \pm 0.12$) in the 2–10 keV band. The energy scale is in the rest system of the observer

6. Discussion

The X-ray spectral properties of Ton S 180 are remarkable when compared with those of classical Seyfert 1s and quasars. First of all, the best fit centroid energy of the iron line and its large equivalent width suggests emission from optically thick ionized matter (e.g. an accretion disk). The properties of iron lines from ionized disks have been studied in detail by Matt et al. (1993, 1996) and Życki & Czerny (1994). The total equivalent width of the line, if the iron is predominantly in the He–like and H–like states, can be much higher (up to more than seven times) than when the iron is neutral (see e.g. Fig. 2 of Matt et al. 1996). This is due to the increased fluorescent yield and the decreased photoelectric absorption opacity. If only the non-scattered component (which is the only one easily detectable) is considered, the EW can be as high as 3 times that of neutral iron. The observed EW, i.e. $\sim$500$\pm$250 eV, is then consistent with the theoretical calculations. The present spectra do not allow us to investigate the line profile in detail. Therefore, in principle the feature at ~ 7 keV could also be the blue horn of a relativistic line from an approximately edge–on accretion disk. It has been proposed that relativistic effects from an approximately edge–on accretion disk could provide the boosting needed to explain the giant-amplitude variability observed in the NLS1

Table 2. LECS+MECS joint fits in the 0.1–10 keV energy range

$F_{1\ keV}$ μJy	Γ_s kT (eV)	E_{break} keV	Γ_h	E_{line} keV	EW eV	χ^2/d.o.f.
2.16	2.68±0.07	$2.5^{+0.5}_{-0.9}$	$2.29^{+0.12}_{-0.19}$	7.11±0.16	507±247	135.0/135
1.95	23^{+18}_{-12}	...	2.48±0.08	7.11±0.14	750^{+240}_{-310}	143.1/135
2.16	2.68±0.07	2.5±0.7	2.16±0.16	...	...	146.0/137
2.20	2.59±0.06	...	...	7.11±0.14	887±310	157.6/137

The absorption column density has been fixed at the Galactic value in all the fits.

IRAS 13224–3809 (Boller et al. 1997). An edge–on disk near a Kerr black hole can also lead to the strong soft X-ray excess often seen in NLS1 (see Cunningham 1975 and the discussion in Sect. 5.1.7 of Boller et al. 1997). A difficulty with this explanation is the observed line equivalent width, which is an order of magnitude larger than expected from an edge–on disk (Matt et al. 1992).

A two-component model provides an adequate description of the continuum X-ray spectrum of Ton S 180, in analogy with several broad lined Seyfert 1s and quasars. However, the slopes of the two components are rather different from those in broad-lined Seyfert 1s (Comastri et al. 1992; Walter & Fink 1993). The soft component is much stronger than in "normal" Seyfert 1s, while the 2–10 keV slope is steeper than the average value observed in Seyfert 1 galaxies (Nandra & Pounds 1994). The increasing evidence for similar behaviour in other NLS1 (Brandt et al. 1997) raises the problem of the origin of such a different spectrum and its relation to the optical properties. The large relative intensity of the soft component, which in Ton S 180 is about a factor 7–8 times greater than the 2–10 keV one, and the steep 2–10 keV slope have important consequences for various models. Even if the observation of a strong iron line suggests that reprocessing is occuring at some level, it appears likely that the strong soft component cannot be due only to disk reprocessing. One would require either highly anisotropic emission or a high energy spectrum extending up to several tens of MeV without any cut–off, at variance with recent high energy observations of Seyferts (e.g. Gondek et al. 1996). The hint of a possible lag of the hard photons with respect to the soft ones (see Sect. 4 and Fig. 2) also argues against disk reprocessing as in this case the soft component is expected to lag the hard one.

A soft X-ray component much stronger than expected from a reprocessing origin alone could lead to a strong Compton cooling of the hot corona electrons and so to a steep hard tail if a significant fraction of the gravitational energy is dissipated in the disk phase. This hypothesis is also supported by the similarities between the X-ray spectra of RE J 1034+393 (Pounds et al. 1995) and Ton S 180, with those of Galactic black hole candidates (GBHC) in their high states. The high states of GBHC are thought to be triggered by increases in the accretion rate resulting in strong thermal emission from a disk accreting at the Eddington limit (e.g. Tanaka 1990; Ebisawa 1991). It is worth noticing that if the black hole is accreting near the Eddington limit, then the disk surface is expected to be strongly ionized, which fits nicely with the present detection of an ionized line. Ionized iron line emission has been recently discovered by ASCA among high luminosity quasars (Nandra et al. 1996,1997), indicating that these sources are radiating at a substantial fraction of the Eddington limit. The present results corroborate the hypothesis of a high L/L$_{Edd}$ ratio in Ton S 180. Note that this is also in agreement with the proposed explanation of the narrow-line Seyfert 1s phenomenon in terms of a high L/L$_{Edd}$ ratio (BBF96; Czerny et al. 1996; Laor et al. 1997): the optical line width will be inversely proportional to L/L$_{Edd}$ if the broad line region is virialized.

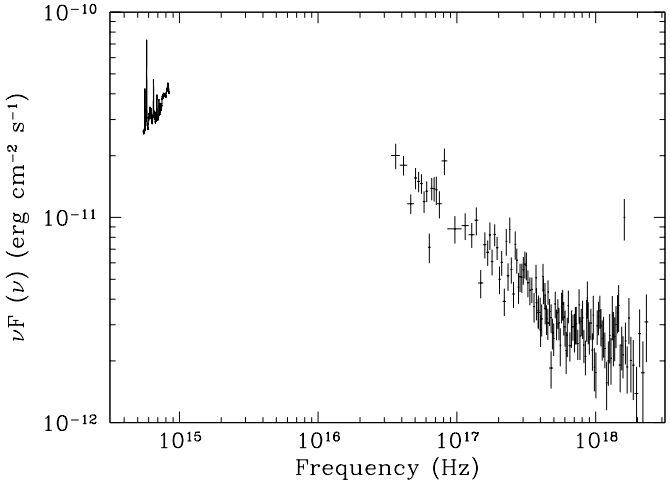

Fig. 5. Spectral energy distribution in the optical and X-ray bands

If the soft X-ray component in Ton S 180 is not the high energy tail of a hot disk accreting at the Eddington limit, but is produced by Comptonization of a lower temperature disk (e.g. Haardt & Maraschi 1993), which would be consistent with the good fit obtained with a power law in the 0.1–2.0 keV range (Table 2), then the origin of the steep 2–10 keV component would remain unexplained, unless a more complicated two temperature comptonizing corona is assumed.

The optical and X-ray spectral energy density distribution is shown in Fig. 5. A simple extrapolation of the data suggest that the energy density peaks somewhere in the extreme ultraviolet, with a behaviour similar to that of other quasars (e.g. Zheng et al. 1997). Also the broad band spectral index α_{ox} = 1.53 between 3000 Å and 2 keV, is close to the average value of 1.56±0.26 of the radio–quiet quasars in the Laor et al. (1997) sample.

Given the large-amplitude variability of Ton S 180, the lack of simultaneous multifrequency observations, and the difficul-

ties that accretion disk models have explaining both the Optical–UV and the soft X-ray emission of AGNs (e.g. Ulrich & Molendi 1995; Siemiginowska et al. 1995; Laor et al. 1997), no attempt has been made to fit the observed spectral energy distribution of Fig. 5 with a disk model.

The link between X-rays and optical properties needs also further examinations. While Ton S 180, similarly to most of the NLS1, displays strong Fe II emission (Fig. 1) and relatively rapid X-ray variability, the other well studied NLS1 RE J 1034+393, with a similar X-ray spectrum and a ionized iron line (Pounds et al. 1995), does not show significant evidences of X-ray variability and displays weaker Fe II lines. The steep 2–10 keV slope coupled with the strong optical Fe II emission in Ton S 180 provide evidence against models of optical Fe II line formation that require flat X-ray spectra and strong hard X-ray emission (e.g. Collin–Souffrin et al. 1988).

Further BeppoSAX observations and coordinated optical campaigns are clearly needed to clarify some of these issues. A more detailed discussion of the X-ray spectral properties of NLS1 is postponed until the observational program is completed.

7. Summary

We have analysed BeppoSAX data and a high-quality optical spectrum of the bright narrow-line Seyfert 1 galaxy Ton S 180. Our main results are the following:

(1) The optical spectrum clearly confirms the NLS1 nature of Ton S 180 and reveals strong Fe II emission. Moreover, the Hα to Hβ ratio, which is one of the lowest measured among AGNs, may imply higher densities than usual in the line emitting region.

(2) Large-amplitude variability of about a factor 2 in both the soft (0.1–3.0 keV) and medium (3.0–10.5 keV) energy ranges has been detected.

(3) The 0.1–10 keV spectrum requires at least two components: (1) a steep $\Gamma \simeq 2.7$ strong soft component below 2 keV which contains a large fraction of the overall energy output, and (2) a weak hard tail with a 2–10 keV slope $\Gamma \simeq 2.3$ that is significantly steeper than the average value found in "normal" Seyfert 1s and quasars.

(4) There is evidence for iron line emission at ~ 7 keV. When fitted with a simple Gaussian, the best fit centroid indicates a high ionization state. Together with the strong soft excess, the steep high energy slope, and the narrow optical lines, these observations suggest that the source is accreting near the Eddington limit and that most of the power is dissipated in the cold disk rather than in the hot corona.

(5) If, alternatively, the observed iron feature is the blue horn of a line produced in a relativistic accretion disk seen edge–on, then significant high amplitude, or even giant, variability is expected due to relativistic boosting effects near the black hole. Optical–UV and X-ray monitoring as well as a broad band deep spectral observation of Ton S 180 appears to be very promising for a better understanding of the physics of NLS1.

Acknowledgements. We thank all the people who, at all levels, have made possible the SAX mission. This research has made use of SAX-DAS linearized and cleaned event files (rev0.1) produced at the BeppoSAX Science Data Center. We thank F. Haardt for useful discussions. AC and GZ acknowledge financial support from the Italian Space Agency under contract ASI–95–RS–152.

References

Boella G., Butler R.C., Perola G.C., et al., 1997a, A&AS 122, 299
Boella G., Chiappetti L., Conti G., et al., 1997b, A&AS 122, 327
Boller T., Trümper J., Molendi S., et al., 1993 A&A 279, 53
Boller T., Brandt W.N., Fink H.H., 1996, A&A 305, 53 (BBF96)
Boller T., Brandt W.N., Fabian A.C., Fink H.H., 1997, MNRAS 289, 393
Brandt W.N., Pounds K.A., Fink H.H. 1995, MNRAS 273, 47P
Brandt W.N., Mathur S., Elvis M., 1997, MNRAS 285, L25
Collin-Souffrin S., Hameury J.M., Joly M., 1988, A&A 205, 19
Comastri A., Setti G., Zamorani G., et al., 1992, ApJ 384, 62
Cunningham C.T., 1975, ApJ 202, 788
Czerny B., Witt H.J., Życki P.T., 1996, in Proceedings of the 2^{nd} Integral Workshop: "The Transparent Universe", St. Malo, France ESA SP–382, 397
Dickey J.M., Lockman F.J., 1990, ARA&A 28, 215
Ebisawa K., 1991, PhD thesis, Tokyo University
Fink H.H., Walter R., Schartel N., Engels D., 1996, A&A 317, 25
Forster K., Halpern J.P., 1996, ApJ 468, 565
Gondek D., Zdziarski A.A., Johnson W.N., et al., 1996, MNRAS 282, 646.
Grupe D., 1996, PhD Thesis, University of Göttingen
Grupe D., Beuermann K., Mannheim K., et al., 1995a, A&A 299, L5
Grupe D., Beuermann K., Mannheim K., et al., 1995b, A&A 300, L21
Haardt F., Maraschi L., 1993, ApJ 413, 507
Hwang C.-Y., Bowyer S., 1997, ApJ 475, 552
Joly M., 1988, A&A 192, 87
Laor A., Fiore F., Elvis M., Wilkes B.J., McDowell J.C., 1997, ApJ 477, 93
Matt G., Perola G.C., Piro L., Stella L., 1992, A&A 257, 63 (Erratum in 263, 453)
Matt G., Fabian A.C., Ross R.R., 1993, MNRAS 262, 179
Matt G., Fabian A.C., Ross R.R., 1996, MNRAS 278, 1111
Nandra K., Pounds K.A., 1994, MNRAS 268, 405
Nandra K., George I.M., Turner T.J., Fukazawa Y., 1996, ApJ 464, 165
Nandra K., George I.M., Mushotzky R.F., Turner T.J., Yaqoob T., 1997, ApJ 488, L91
Osterbrock D.E., Pogge R.W., 1985, ApJ 297, 166
Otani C., Kii T., Miya K., 1996, in Proceedings of: "Röntgenstrahlung from the Universe" MPE Report 263, 491
Parmar A.N., Martin D.D.E., Bavdaz M., et al., 1997, A&AS, 122, 309
Phillips M.M., 1976, ApJ 208, 37
Pounds K.A., Done C., Osborne J.P. 1995, MNRAS 277, L5
Rees M.J., Netzer H., Ferland G.J. 1989, ApJ 347, 640
Rodríguez-Pascual P.M., Mas-Hesse J.M., Santos-Lleó M. 1997, A&A 327, 72
Ross R.R., Fabian A.C., Brandt W.N. 1996, MNRAS 278, 1082
Siemiginowska A., Kuhn O., Elvis M., et al., 1995, ApJ 454, 77
Tanaka Y., 1990, in Hunt J., Battrick, B., eds., 23rd ESLAB Symp. on X-ray Astronomy, ESA SP–296, p. 3
Ulrich M.-H., Molendi S. 1995, A&A 293, 641
Vennes S., Polomski E., Bowyer S., Thorstensen J.R., 1995, ApJ 448, L9
Walter R., Fink H.H., 1993, A&A 274, 105
Winkler H., Glass I.S., van Wyk F., et al. 1992, MNRAS 257, 659
Życki P.T., Czerny B., 1994, MNRAS 266, 653
Zheng W., Puetter R.C., 1990, ApJ 361, 40
Zheng W., Kriss G.A., Telfer R.C., Grimes J.P., Davidsen A.F., 1997, ApJ 475, 469